

***In-Situ* Corrosion Monitoring of Scratched Epoxy Coated Carbon Steel in Saturated Ca(OH)₂ with or without 3% NaCl by Scanning Electrochemical Microscopy and Electrochemical Impedance Spectroscopy**

Thangaraj Balusamy, Toshiyasu Nishimura*

Corrosion Resistant Steel Group, Research Center for Structural Materials (RCSM), National Institute for Materials Science, Tsukuba, Japan
Email: *NISHIMURA.Toshiyasu@nims.go.jp

Received 4 May 2016; accepted 27 June 2016; published 30 June 2016

Copyright © 2016 by authors and Scientific Research Publishing Inc.
This work is licensed under the Creative Commons Attribution International License (CC BY).
<http://creativecommons.org/licenses/by/4.0/>



Open Access

Abstract

The present work is investigated the *in-situ* monitoring of local corrosion process of scratched epoxy coated carbon steel in saturated Ca(OH)₂ with and without 3% NaCl using SECM and correlated with EIS. The results obtained from EIS analysis showed that the corrosion resistance of scratched epoxy coated carbon steel decreases in Cl⁻ containing solution as the increase in wet/dry corrosion cycles. This was indicated by decrease in film resistance (R_f) and charge transfer resistance (R_{ct}), while the coated steel maintain the resistance values in saturated Ca(OH)₂, most of which recovered after drying. The corrosion process was monitored using SECM by setting the tip potential at -0.70 V vs Ag/AgCl, where the consumption of dissolved oxygen occurred at the surface of test sample. The consumption of dissolved oxygen current (I'_{oxy-c}) values was increased during the immersion in a solution with 3% NaCl. However, in wet/dry corrosion cycles, I'_{oxy-c} was decreased due to the coverage of hydroxides/oxides at scratch area which suppressed the consumption of dissolved O₂. It was found that the continuous decrease in corrosion was mainly attributed to continuous formation of corrosion products at anodic spots.

Keywords

Epoxy Coated Carbon Steel, Alkaline Solution, Chlorides, SECM, Wet/Dry Corrosion Cycles

*Corresponding author.

1. Introduction

Scanning electrochemical microscopy (SECM) has been paid much attention in corrosion research to probe the local corrosion process with a high spatial resolution. In SECM, the corrosion process can be acquired in real time and *in-situ* manner to explore the corroborative evidence for corrosion mechanisms [1]-[5]. In addition, the usage of electrochemical mediators in SECM may interfere the electrochemical reactions during corrosion process. For an alternative, substrate generation-tip collection (SG-TC) mode of SECM has been introduced to monitor the electro active species already present in the electrolyte [4] [5]. Under the open circuit potential, the anodic process (metal dissolution reaction) is balanced by the cathodic process of oxygen reduction reaction occurred on the steel surface [5] [6]. Hence, the anodic and cathodic processes can be monitored successfully using SECM, and it has advantage on finding the chemical selectivity of the corrosive species as compared to other localized techniques [7] [8].

Souto *et al.* [1] has studied the degradation of paint coating without an artificial defect by SECM, immersed in Cl^- and Cl^- free sulphate solution. They found that the corrosion initiation and degradation of coating occurred via blistering at early stage in Cl^- containing solution as compared to Cl^- free sulphate solution. They have also mentioned that the formation of blister was not caused the complete damage of organic coating and it needs further depth investigation. Moreover, organic coating with considerable artificial defect was also studied by Souto *et al.* [4] in solutions of 0.1 M KCl, 0.1 M K_2SO_4 and 0.1 M $\text{Na}_2\text{B}_4\text{O}_7$ using SECM. The results revealed that the coating degradation occurred at delamination front (borders of defect), while the metal surface at defect was almost unaffected from corrosion in 0.1 M $\text{Na}_2\text{B}_4\text{O}_7$. However, the corrosion degradation was detected at defects in 0.1 M KCl and 0.1 M K_2SO_4 solutions and it was reduced by the formation of corrosion products as increase the immersion duration [4]. Recently, Schachinger *et al.* [9] reported that ionic species such as Na^+ , SO_4^{2-} and CO_3^{2-} are necessary to initiate the blistering of organic coating and the presence of oxidizing species (sodium percarbonate) enhanced the blister growth enormously. Nguyen and Martin [10] depicted that coating with considerable artificial defect exhibits the coating degradation through anodic blistering at near and along the artificial defects and cathodic delamination around the anodic blisters away from the defects. However, the coated steel surface with artificial defects remained un-corroded during exposure even in sat. $\text{Ca}(\text{OH})_2$ containing 0.6 M NaCl (3.5% NaCl). It raise the following questions to be answered: 1) if considerable artificial defect (scratch) is present, what extent of local corrosion attack could occur at scratch area, 2) whether the coating degradation occurs during immersion under such conditions, 3) what is the extent of corrosion at near the scratch and away from the scratch under immersion and wet/dry corrosion conditions, if any. A better understanding on these aspects is important to explore the onset of corrosion and coating degradation in sat. $\text{Ca}(\text{OH})_2$ containing 3% NaCl.

Epoxy based protective coatings have been applied to the steels against corrosion for many years which acts as a physical barrier layer against corrosion and cost effective [11]-[13]. The majority of coated steels and their corrosion performance were conducted in NaCl solutions. There is a limited published literature in higher pH solution by *in-situ* measurements on the understanding of corrosion mechanism of steels [2] [14] [15]. The corrosion behavior of scratched epoxy coated carbon steel in sat. $\text{Ca}(\text{OH})_2$ with 3% NaCl using SECM is not reported previously under immersion and wet/dry corrosion cycles. Moreover, the corrosion mechanism is a quite complex process in scratched and coated area of the epoxy coated carbon steel in sat. $\text{Ca}(\text{OH})_2$ containing Cl^- ions and depends on the type of metal/alloy, its chemical composition and ability to form a passive film, defect size, concentration of Cl^- ions, pH, transport phenomena and the nature of corrosion products [16]. Hence, in the present study, an attempt is made to understand and monitor the local corrosion process of scratched epoxy coated carbon steel in sat. $\text{Ca}(\text{OH})_2$ with and without 3% NaCl using SECM. Electrochemical impedance spectroscopy (EIS) is also performed on the epoxy coated carbon steel with artificial cross cuts in both test solution for 15 days of wet/dry corrosion cycles and correlated with SECM results. Moreover, the inferences made in this study are likely to provide a better insight on the local corrosion mechanism of scratched epoxy coated carbon steel in chloride containing solution during immersion and wet/dry corrosion cycles. We also proposed a graphical model to understand the degradation of coating and steel corrosion in bulk solution as well as wet/dry corrosion cycles test conditions.

2. Experimental Details

2.1. Preparation of Specimens

The chemical composition of the carbon steel specimen was 0.1C-0.3Si-0.7Mn-0.01P-0.003S-0.03Al-0.003N-

0.002 O-balance Fe (in mass %) as per JIS-SM (Japanese industrial standards-sheet metal). The carbon steel specimens (0.5 mm thick), with the surface areas of $17 \times 17 \text{ cm}^2$ and $1.7 \times 1.7 \text{ cm}^2$ were abraded by silicon carbide (SiC) emery papers up to 800 grit. And then, the specimens were rinsed with distilled water and dried well in compressed air, and further cleaned with ethanol prior to coating.

2.2. Preparation of Coatings and Electrolyte

The organic coating used in this investigation was commercially available fast drying epoxy. The liquid epoxy resin was a blend made of multifunctional low molecular weight diluents and diglycedal ether of bis-phenol-A and the curing agent was the aliphatic amines. The weight ratio of the epoxy resin to the curing agent was 2:1. The epoxy resin was coated using a drawdown bar at a constant speed and then kept at room temperature for 24 h. This led to the formation of uniform coating with thickness of $40 \mu\text{m}$. An artificial scratch on the epoxy coating was produced by using a driller, and the dimension of scratch was of $1000 \mu\text{m}$ width and 10 mm length used for the SECM measurements. While the artificial scratches with diameter of $150 - 200 \mu\text{m}$ of crosscuts were used for EIS measurements. The specimens were then exposed to aerated aqueous solutions of saturated $\text{Ca}(\text{OH})_2$ with and without 3 % of NaCl. The test electrolyte was prepared by using the analytical grade chemicals then filtered using Whatman 42 filter paper for SECM measurements.

2.3. EIS Measurements

A wet/dry corrosion cyclic test was conducted by wetting the specimens in 0.4 L/m^2 in sat. $\text{Ca}(\text{OH})_2$ with and without 3% NaCl solutions for 12 h exposure. And then the specimens were dried in a chamber maintained at 25°C , 60% RH for 12 hs. Prior to the exposure in to the test solution, the specimens were washed in distilled water and dried well to prevent the progressive salt accumulation. EIS measurements were carried out periodically in sat. $\text{Ca}(\text{OH})_2$ with and without 3% NaCl solution. The EIS test was performed in a two-electrode cell, using coated steel with crosscuts as a working electrode and the same type of electrode was used as a counter electrode. A frequency response analyzer (IVIUMSTAT: Electrochemical Interface, Ivium Technologies, The Netherlands) was used for EIS measurements with amplitude of 10 mV over a frequency range of 20 kHz to 1 mHz. All the electrochemical measurements were carried out at room temperature (25°C) at their open circuit potentials (OCPs). Prior to the EIS measurements, the scratched epoxy coated carbon steels were immersed in the test solution for an h until their open circuit potential (OCP) stabilized. The obtained EIS experimental data were analyzed by ZSimpwin software.

2.4. SECM Measurements

The SECM experiments were performed using SECM (UniScan SECM 370 model) with PG580R bi-potentiostats controlled by a computer. A Pt microelectrode tip (SECM-tip) with a $25 \mu\text{m}$ diameter was used to probe the local electrochemical response. The system was operated by a three-electrode configuration since the scratched epoxy coated carbon steel was used as a working electrode (WE) and it was left unbiased during experiments and kept in its corresponding OCPs. An Ag/AgCl/(sat. KCl) electrode and Pt strip was used as a reference electrode and counter electrode respectively. The SECM-tip was held at -0.70 V vs Ag/AgCl/(sat. KCl), where the electro-reduction of dissolved oxygen (Equation (1)) could be the principle reaction and it can be monitored by SECM.



The distance between WE and SECM-tip was fixed about $50 \mu\text{m}$ and the relative location of the SECM-tip to the WE was monitored by the camera system, which can be adjusted by a stepper motor in the x, y and z directions. Scratched epoxy coated specimens were mounted horizontally facing upwards in the corrosion Tri-cell. SECM scans were conducted parallel to the specimen surface. The SECM-tip was cleaned prior to testing by cyclic voltammetry (CV) in sat. $\text{Ca}(\text{OH})_2$ with and without 3% NaCl solution at the scan rate of 20 mV/s [2]. The SECM 3D scanning was performed at $7000 \times 2000 \mu\text{m}^2$ area by moving of SECM-tip at constant height ($50 \mu\text{m}$ -z axis). The step size (50 and $100 \mu\text{m}$ in x-y direction) was controlled to obtain a 3D plot of 71×11 lines in the x-y directions. The higher size of SCEM images ($7000 \times 2000 \mu\text{m}^2$) were used in the present study for better insight on local corrosion at scratch as well as coating area. The experiments were conducted at different immersion time for about 1 - 7 h. The SECM line scan profiles were taken from SECM 3D scan profile to have a

better insight. The same specimen has been kept for wet/dry corrosion cycles (1 - 4 days) without disturbing the corrosion cell. After each wet/dry cycles the specimens were cleaned with distilled water to remove the salt deposition on scratched epoxy coated carbon steel and the experiments was carried out at same manner. Similarly, SECM-tip was also cleaned carefully after each wet/dry corrosion cycles. The dilute H_2SO_4 was used to remove the deposits and washed with distilled water by adjusting x and z directions using stepper motor, while the relative locations were carefully maintained.

3. Results and Discussion

3.1. Wet/Dry Corrosion Performance of Scratched Epoxy Coated Carbon Steel by EIS

Wet/dry corrosion cycle performance of scratched epoxy coated carbon steel was carried out in sat. $Ca(OH)_2$ with and without 3% NaCl by EIS measurements at their respective OCPs. The obtained EIS results were characterized by Nyquist and Bode plots of scratched epoxy coated carbon steel in sat. $Ca(OH)_2$ with and without 3% NaCl as shown in **Figure 1** and **Figure 2**. It was evident from **Figure 1** and **Figure 2**, there was a two resistance parts one in a high frequency corresponds to the coating behavior and the other one in low frequency part related to charge transfer resistance of the corroding of carbon steel. The obtained EIS data was used to fit an equivalent electrical circuit model as shown in **Figure 3**. In this circuit model, R_s represents the solution resistance while CPE_f and R_f correspond to the film capacitance and film resistance respectively. The R_{ct} and CPE_{dl} are the charge transfer resistance and double layer capacitance of the corroding steel, respectively. The impedance of CPE is given by $Z_{CPE} = 1/Q(j\omega)^n$, where “ n ” is the CPE exponent. The capacitance element Q (CPE) will be pure capacitance when $n = 1$ while it will be pure resistance when $n = 0$. Q is called as CPE when $0.5 < n < 1$ and it prevails under conditions of surface heterogeneity. The electrochemical parameters derived after fitting the EIS data are shown in **Figures 4(a)-(d)**. The value of “ n ” lies between 0.5 and 0.98 in sat. $Ca(OH)_2$ with and without

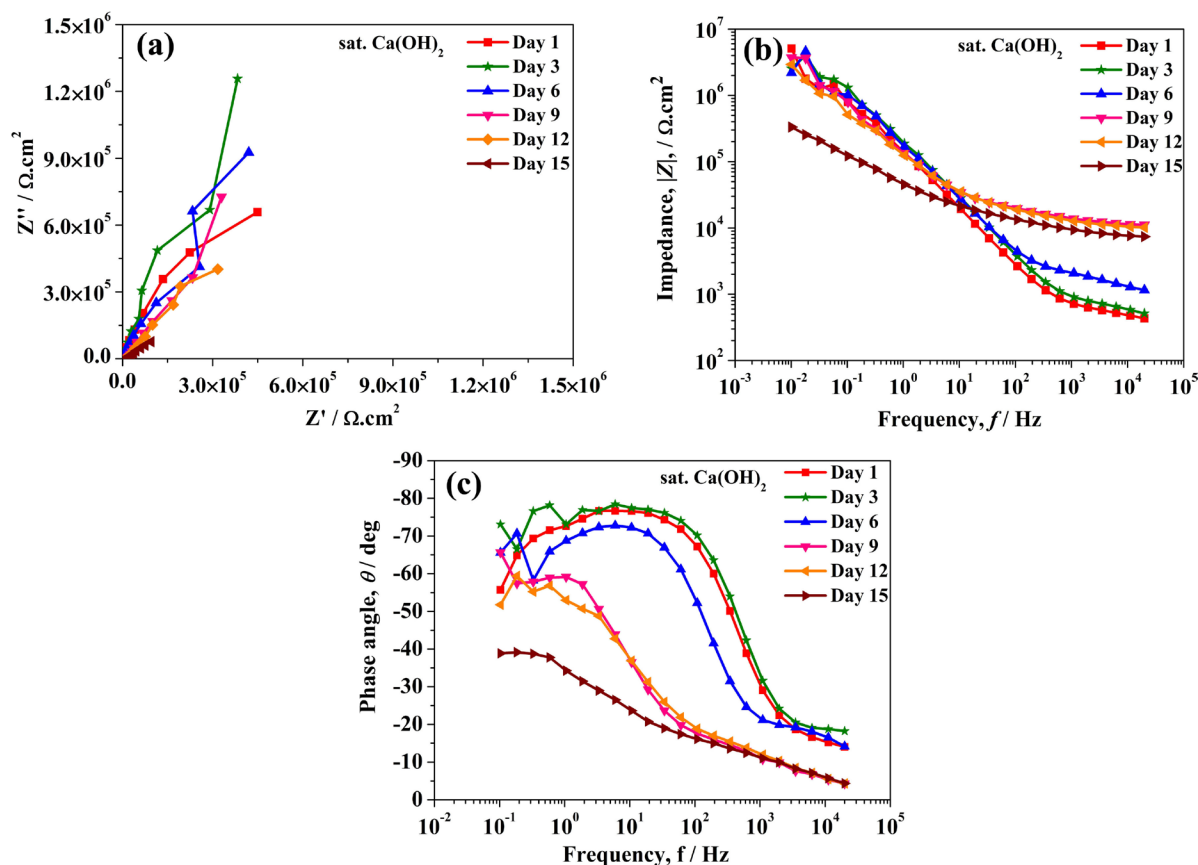


Figure 1. Nyquist (a), Bode impedance (b) and Bode phase angle (c) plots of scratched epoxy coated carbon steel after wet/dry corrosion cycles test in sat. $Ca(OH)_2$ at their respective OCPs.

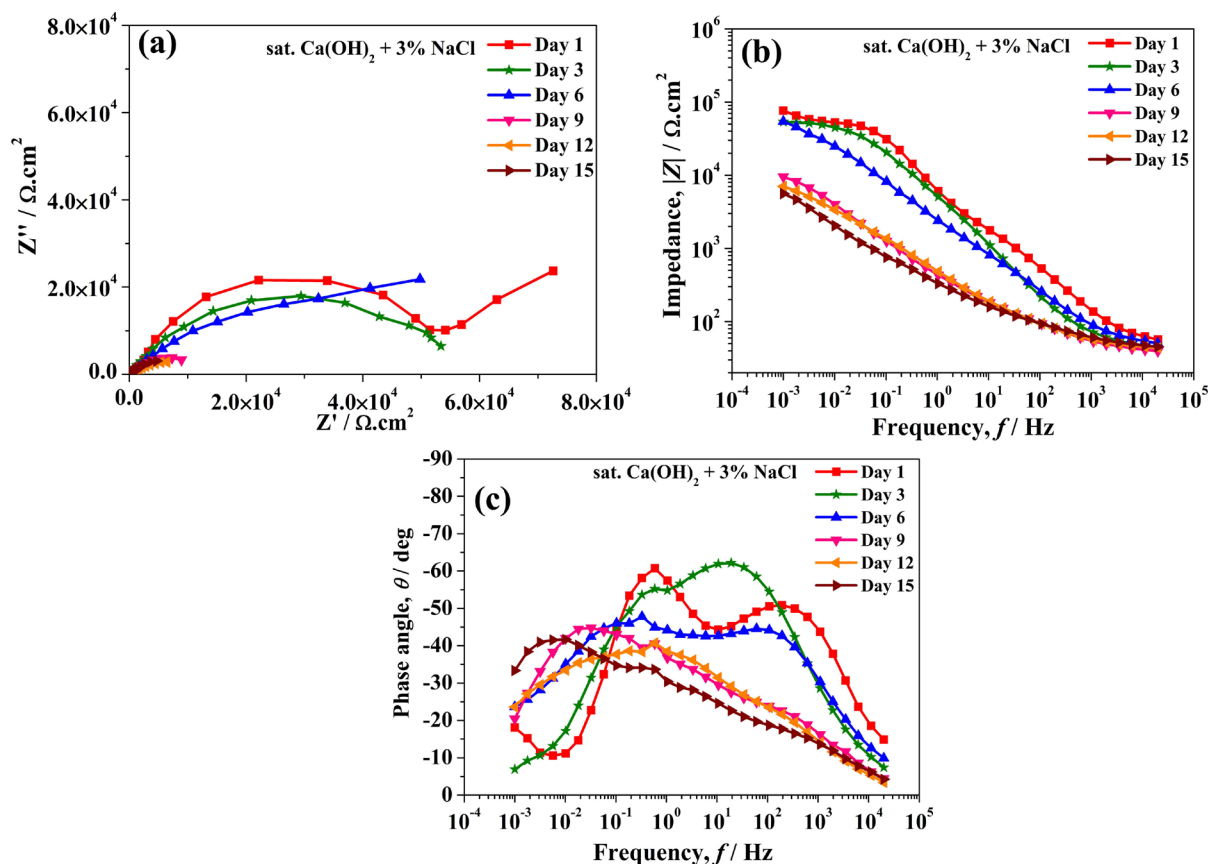


Figure 2. Nyquist (a), Bode impedance (b) and Bode phase angle (c) plots of scratched epoxy coated carbon steel after wet/dry corrosion cycles test in sat. $\text{Ca}(\text{OH})_2$ with 3% NaCl at their respective OCPs.

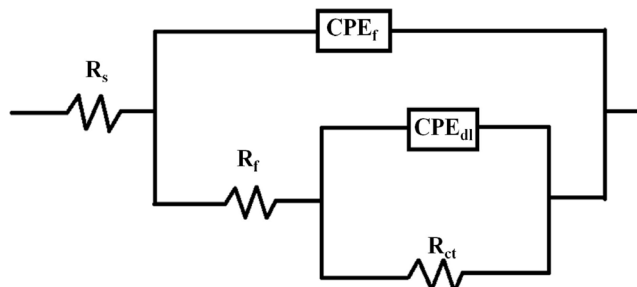


Figure 3. Equivalent circuit diagram for scratched epoxy coated carbon steel after wet/dry corrosion cycles test in sat. $\text{Ca}(\text{OH})_2$ and sat. $\text{Ca}(\text{OH})_2$ containing 3% NaCl for various days.

3% NaCl, the choice of CPE as the circuit element seems to be appropriate. For the better comparison, the same electrical circuit model has been used for the all cases in the present study. The solution resistance, R_s of the system was constant ($35 - 47 \Omega \cdot \text{cm}^2$) for sat. $\text{Ca}(\text{OH})_2$ containing 3% NaCl exposed for 15 days after wet/dry corrosion cycles test, while R_s of the system was varied from $348 - 1017 \Omega \cdot \text{cm}^2$ for sat. $\text{Ca}(\text{OH})_2$. The film resistance, R_f of scratched epoxy coated carbon steel was almost constant for 7 days (1.32 to $2.12 \text{ k}\Omega \cdot \text{cm}^2$) of wet/dry corrosion cycles test in sat. $\text{Ca}(\text{OH})_2$. Upon increase in wet/dry cycles, increase in film resistance (R_f) was observed from 2.12 to $15.22 \text{ k}\Omega \cdot \text{cm}^2$ and it maintained the resistance values for 15 days (Figure 4(a)) with the corresponding decrease in film capacitance, CPE_f (Figure 4(b)) from 1.02×10^{-6} to $1.39 \times 10^{-7} \text{ S} \cdot \text{s}^n \cdot \text{cm}^{-2}$. On the other hand, the charge transfer resistance, R_{ct} (Figure 4(c)) of corroded steel was decreased marginally from 2.42 to $0.77 \text{ M}\Omega \cdot \text{cm}^2$ with corresponding increases in double layer capacitance, CPE_{dl} (Figure 4(d)) from 4.54×10^{-7} to $6.19 \times 10^{-6} \text{ S} \cdot \text{s}^n \cdot \text{cm}^{-2}$ in absence of Cl^- ions. The film resistance, R_f of the scratched epoxy coated carbon

steel was decreased from 1.0 to 0.14 $\text{k}\Omega\cdot\text{cm}^2$ upon increase in wet/dry corrosion cycles test in sat. $\text{Ca}(\text{OH})_2$ containing 3% NaCl. The corresponding film capacitance (CPE_f) was increased from 2.40×10^{-5} to 5.83×10^{-4} $\text{S}\cdot\text{s}^n\cdot\text{cm}^{-2}$. The R_{ct} values of corroding steel in 3% NaCl were decreased to large extent form $61.19 \text{ k}\Omega\cdot\text{cm}^2$ to $4.48 \text{ k}\Omega\cdot\text{cm}^2$ (Figure 4(c)) with corresponding increase in CPE_{dl} from 1.28×10^{-5} to 1.14×10^{-3} $\text{S}\cdot\text{s}^n\cdot\text{cm}^{-2}$ (Figure 4(d)). It was observed that with the addition of 3% NaCl in to the sat. $\text{Ca}(\text{OH})_2$ leads to the continuous decrease in corrosion resistance of scratched epoxy coated carbon steel as compared to in sat. $\text{Ca}(\text{OH})_2$ (Figure 4).

The photographs taken after wet/dry corrosion cycles tests of scratched epoxy coated carbon steel in sat. $\text{Ca}(\text{OH})_2$ and sat. $\text{Ca}(\text{OH})_2$ containing 3% NaCl is shown in Figure 5. It can be seen from Figure 5 that the occurrence of corrosion damage at along with and away from the scratch (arrow marks in Figure 5(b)) and severe

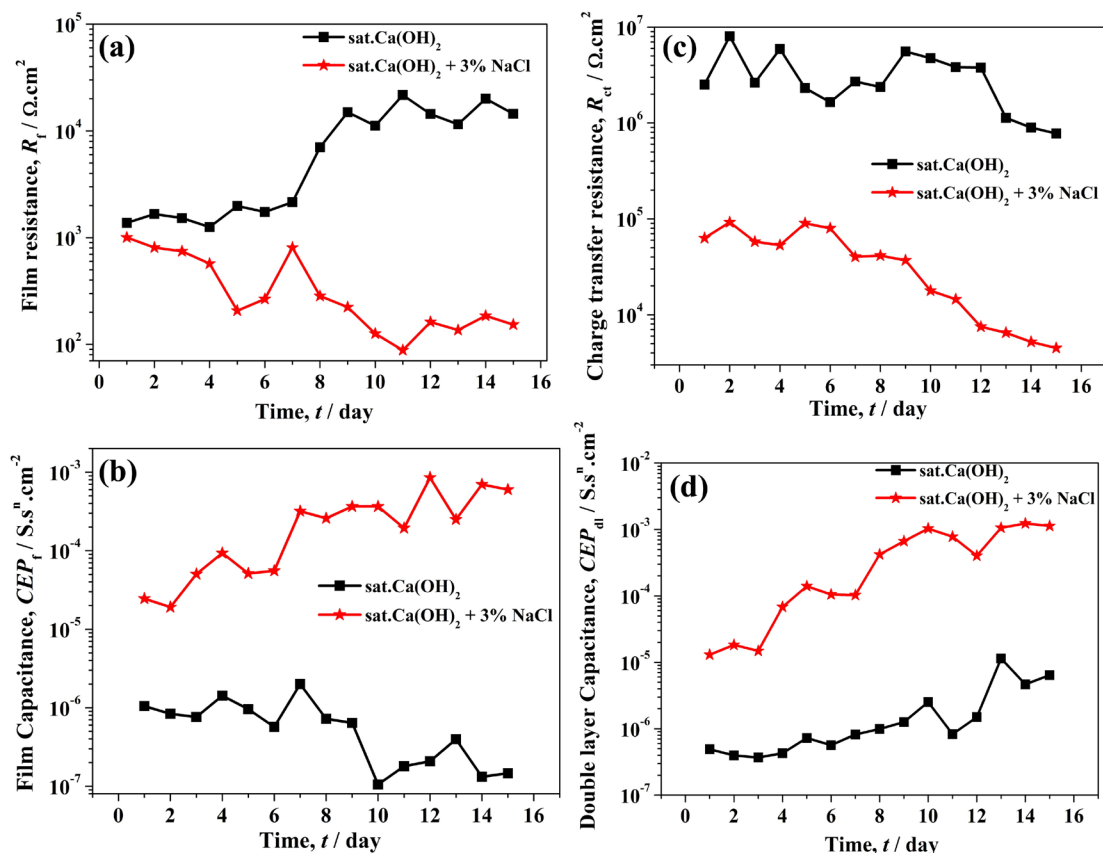


Figure 4. Impedance values of (a) R_f , (b) CPE_f , (c) R_{ct} and (d) CPE_{dl} for scratched epoxy coated carbon steel after wet/dry cycles test in sat. $\text{Ca}(\text{OH})_2$ and sat. $\text{Ca}(\text{OH})_2$ containing 3% NaCl recorded at their respective OCPs for various days.

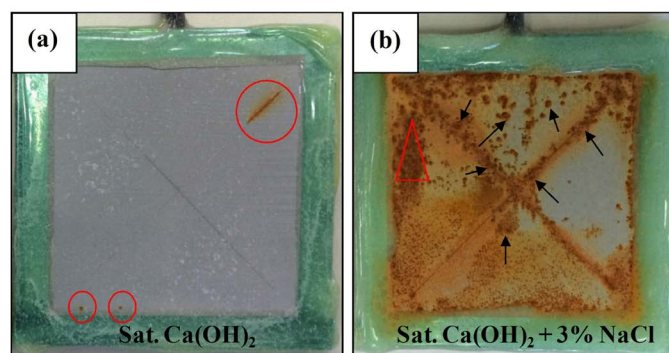


Figure 5. Photographs of scratched epoxy coated carbon steel after wet/dry corrosion cycles test for 15 days: (a) In sat. $\text{Ca}(\text{OH})_2$; (b) In sat. $\text{Ca}(\text{OH})_2$ containing 3% NaCl.

corrosion damage after wet/dry corrosion cycles test in Cl^- containing solution. Blister formation is the first indication of organic coatings failure due to undercoating corrosion, which initiates the delamination of coating from metallic substrates. The blister formation was due to osmotic pressure difference by water uptake of coating which acts as a semi permeable membrane where the diffusion of Cl^- ions and oxygen could occur at the coating-substrate interface that eventually delaminate the coating. It was reported that permeation of oxygen and Cl^- ions leads to the formation of corrosion products (anodic zones) at center of the blister, while increase of pH at the edges of the blister causing delamination of the coating [9]. The additional formation of blisters lead to the extent of corrosion damage of coating along with already formed blisters (marked as a triangle in **Figure 5(b)**). This is due to the fact that penetration of Cl^- ions as well as water uptake of coating leads to the additional pathways for corrosion degradation due to the blistering during wetting cycles. The continuous increase in blisters as well as corrosion at already formed blisters results in the continuous decrease in corrosion resistance of scratched epoxy coated carbon steel in sat. $\text{Ca}(\text{OH})_2$ with 3% NaCl. This was clearly indicated by decrease in R_f with corresponding increase in CPE_f as well as R_{ct} and CPE_{dl} in **Figure 4** respectively. On the other hand, a few corrosion attacks were observed in sat. $\text{Ca}(\text{OH})_2$ along with the scratch and coated area (marked as a circles in **Figure 5(a)**). These inferences supports that the coating properties were not changed much during wet/dry corrosion cycles in sat. $\text{Ca}(\text{OH})_2$. This might be due to the fact that recovery of coating properties after dry cycles [10]. However, the marginal decrease in R_{ct} with corresponding increase in CPE_{dl} is observed. These results suggest that the observation made by visually from **Figure 5** support the change in impedance parameters in **Figure 1** and **Figure 2** and **Figure 4**.

Hence, the results obtained from EIS and visual observation, the decrease in corrosion resistance was attributed to the corrosion at scratch as well as blister formation along with scratch and away from the scratch in Cl^- containing solution in initial wet/dry corrosion cycles. However, the formation blisters along with scratch as well as away from the scratch during wet/dry cycles in sat. $\text{Ca}(\text{OH})_2$ with 3% NaCl is the main responsible for continuous decrease in corrosion resistance of scratched epoxy coated carbon steel. Thus, the corrosion degradation at the scratch area is limited due to the formation of corrosion products (partially protected) upon increase in wet/dry cycles. The continuous increases in wet/dry cycles lead to the formation of additional blisters during wetting the specimen. The blister rupture could also occur due to repeated expansion-contraction during wet/dry corrosion cycle. This has been visually observed in **Figure 5(b)** and also noted the formation of corrosion spots on the scratched epoxy coated carbon steel after 15 days of wet/dry corrosion cycles in sat. $\text{Ca}(\text{OH})_2$ containing 3% NaCl. For better understanding on the coating degradation (blister formation) and steel corrosion of scratched epoxy coated carbon steel, the corrosion experiments have been conducted using SECM in sat. $\text{Ca}(\text{OH})_2$ and sat. $\text{Ca}(\text{OH})_2$ containing 3% NaCl. Since, SECM have advantage on the chemical selectivity of corrosive species (electro active species already present in solution such as oxygen) involved on the local corrosion process which provides better insight on the local corrosion mechanism of scratched epoxy coated carbon steel.

3.2. SECM Measurements of Scratched Epoxy Coated Carbon Steel

The changes in topographic information and electrochemical activity at the surface of scratched epoxy coated carbon steel have been acquired from SECM 3D maps by *in-situ* manner in sat. $\text{Ca}(\text{OH})_2$ and sat. $\text{Ca}(\text{OH})_2$ containing 3% NaCl. For the better insight, the corresponding SECM line scans have been analyzed from SECM 3D maps. The dissolved oxygen was considered as a mediator and monitored by setting the SCEM-tip potential at -0.70 V vs. $\text{Ag}/\text{AgCl}/(\text{sat. KCl})$ at their respective OCPs for 1 - 7 h immersion in sat. $\text{Ca}(\text{OH})_2$ and sat. $\text{Ca}(\text{OH})_2$ containing 3 % NaCl [4] [5]. On the other hand, the wet/dry corrosion cycle performance was carried out for same specimens for 1 - 4 days in both test solutions. The change in 3D tip current distribution has been acquired over the coating as well as at scratch area of epoxy coated carbon steel. The results obtained from SECM analysis has been correlated with wet/dry corrosion cycles test results performed by EIS and discussed.

3.2.1. SECM Analysis by Immersion Test

SECM 3D surface topographic images of scratched epoxy coated carbon steel in sat. $\text{Ca}(\text{OH})_2$ containing 3% NaCl exposed for 1, 3, 5 and 7 h at the tip potential of -0.70 V were shown in **Figure 6**. It was evident from **Figure 6**, the tip current distribution ($7000 \times 1200 \mu\text{m}^2$ in x and y directions, $50 \mu\text{m}$ in z direction) obtained over the scratched epoxy coated carbon steel for the measurement of dissolved oxygen in sat. $\text{Ca}(\text{OH})_2$ containing 3% NaCl. The decrease in tip current could be observed when the SECM tip scanned over the scratch area. This be-

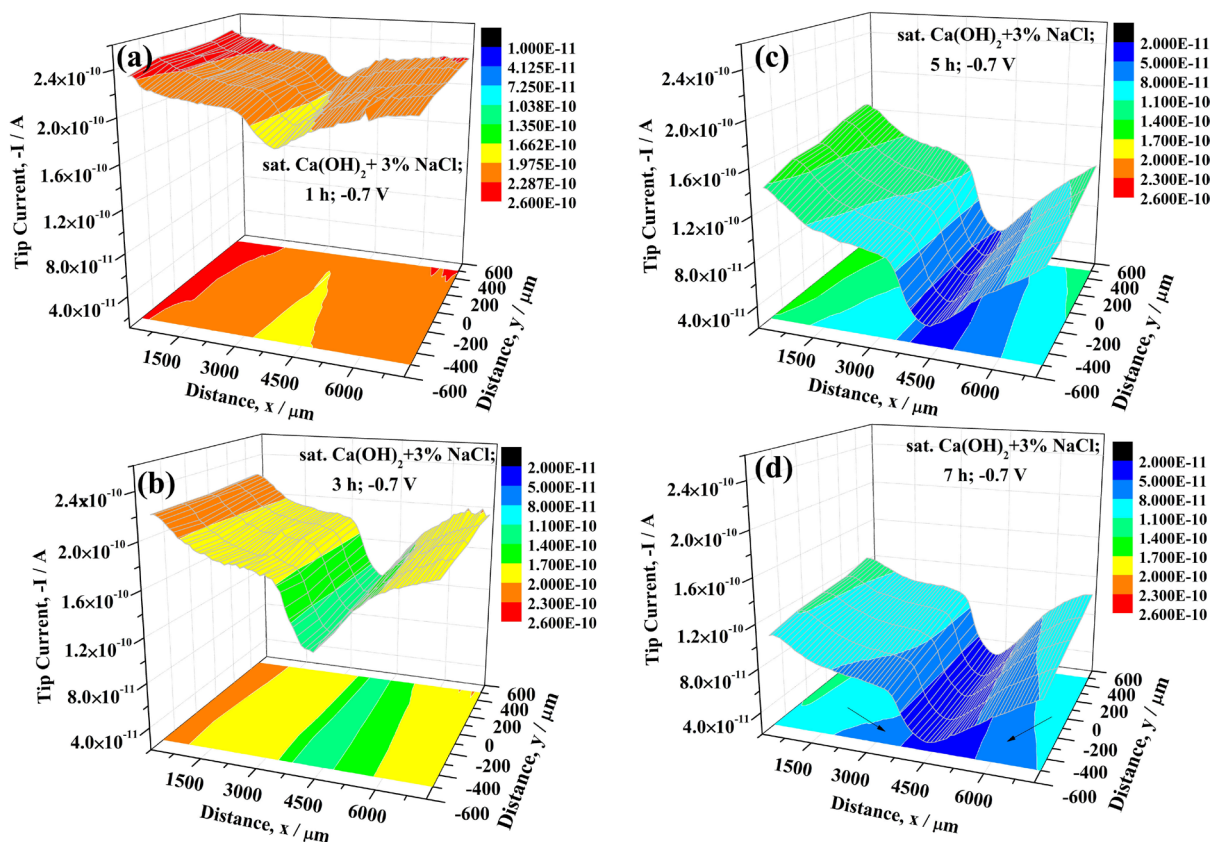


Figure 6. SECM topographic images of scratched epoxy coated carbon steel in sat. $\text{Ca}(\text{OH})_2$ containing 3% NaCl: (a) 1 h; (b) 3 h; (c) 5 h and (d) 7 h at the tip potential of -0.70 V vs. $\text{Ag}/\text{AgCl}/\text{sat. KCl}$. The images represent the $7000 \mu\text{m} \times 1200 \mu\text{m}$ in x and y directions. The vertical z direction is the tip current.

havior was attributed to the consumption of dissolved oxygen at cathodic sites (by Equation (1)) of scratched steel surface. The continuous decreases in tip current from -0.187 to -0.025 nA (nearly one fold decrease) was observed for 1 - 7 h immersion, while the decrease in tip current distribution was widened with higher immersion time. This observation clearly implies that corrosion rate has been enhanced at scratch area with immersion time by the addition of Cl^- ions in to sat. $\text{Ca}(\text{OH})_2$.

For better insight, the corresponding SECM line scans for 1 - 7 h immersion is shown in Figure 7. It is seen clearly from Figure 7 that the large extent of decrease in tip current was observed at scratch for 1 - 4 h immersion in sat. $\text{Ca}(\text{OH})_2$ containing 3% NaCl, while change in tip current was less extent with increase in immersion time. This clearly pointed out the consumption of dissolved oxygen at cathodic microcells originated from the steel surface (scratched area). Further, the shape of the curves is broadened after 4 h immersion, which shows the cathodic reactions are shifted to the scratch front. These observation reveals the formation of corrosion products (such as $\text{Fe}(\text{OH})_2$ or $\text{Fe}(\text{OH})_3$ at high pH) at scratch area, which suppress the consumption of dissolved oxygen at scratch area and extent the cathodic reaction to the scratch front leads to cathodic delamination. This has been clearly noticed in 3D scans that the extent of shift of decrease in tip current distribution at the scratch front (arrow marks shown in Figure 6(d)) for 7 h immersion in sat. $\text{Ca}(\text{OH})_2$ with 3% NaCl. On the other hand, experiments are also conducted in sat. $\text{Ca}(\text{OH})_2$ for better comparison to the sat. $\text{Ca}(\text{OH})_2$ with 3% NaCl. SECM 3D maps and SECM line scan profiles shows very small change in tip current values over the scratched area (Figures not shown). However, the line scans analyses have been carried out as like shown in Figure 7 and the tip current values were taken at scratch area. The tip current values at scratched area were slightly high in sat. $\text{Ca}(\text{OH})_2$ for entire duration of immersion (1 - 7 h), which was exactly opposite trend observed in sat. $\text{Ca}(\text{OH})_2$ containing 3% NaCl for 1 - 7 h.

The quantitative analyses of consumption of dissolved oxygen currents ($I_{\text{oxy-c}}$ and $I'_{\text{oxy-c}}$) at the scratch area was analyzed by subtracting the tip current values from I_1' (considered as a tip current equal to over coating) to

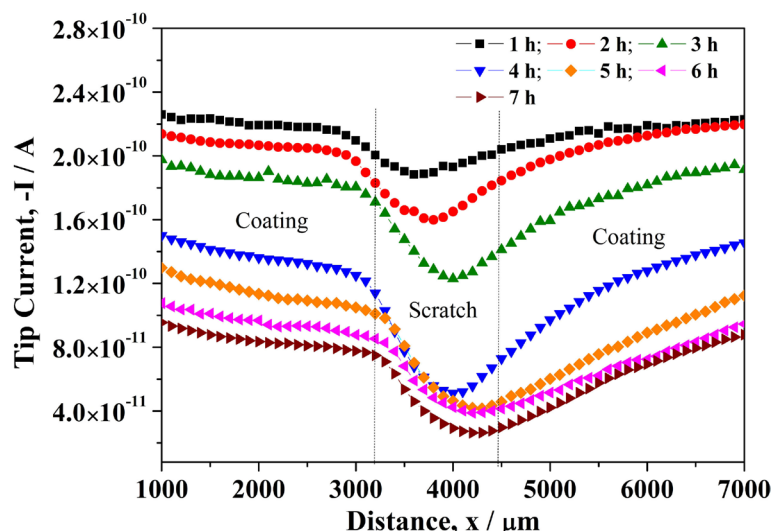


Figure 7. SECM line scans of scratched epoxy coated carbon steel in sat. $\text{Ca}(\text{OH})_2$ containing 3% NaCl at the tip potential of -0.70 V vs. Ag/AgCl/sat.KCl.

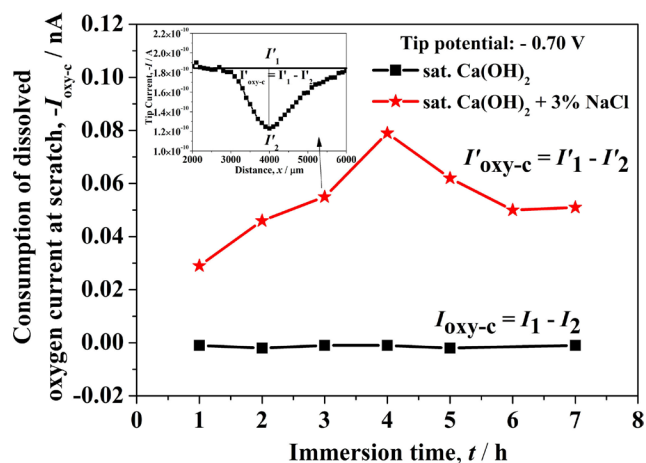


Figure 8. Consumption of dissolved oxygen currents ($I_{\text{oxv-c}}$ and $I'_{\text{oxv-c}}$) measured over scratched epoxy coated carbon steel in sat. $\text{Ca}(\text{OH})_2$ and sat. $\text{Ca}(\text{OH})_2$ containing 3% NaCl as a function of immersion time at the tip potential of -0.70 V vs. Ag/AgCl/sat.KCl respectively.

I'_2 as shown in inset **Figure 8** in sat. $\text{Ca}(\text{OH})_2$ with and without 3% NaCl respectively. In the case of $\text{Ca}(\text{OH})_2$ containing 3% NaCl, the increase in $I'_{\text{oxv-c}}$ from -0.027 to -0.079 nA for 1 to 4 h immersion and starts to decrease from -0.079 to -0.049 nA for 4 - 7 h immersion. This clearly implies that the local corrosion process is active up to 4 h immersion from 1 h due to continuous consumption of dissolved oxygen at cathodic sites originated from steel surface (scratch area). After 4 h immersion, the consumption of dissolved oxygen was slightly reduced. This behavior was thought due to the formation of hydroxides ($\text{Fe}(\text{OH})_2$ or $\text{Fe}(\text{OH})_3$) at scratch, because the dissolved Fe^{2+} from steel was easily to combine with OH^- ions in a high pH solution. In addition, tip current distribution or tip current at scratch area has been widened after 4 h immersion (**Figure 6(d)** and **Figure 7**). This was mainly attributed to the formation of hydroxides ($\text{Fe}(\text{OH})_2$ or $\text{Fe}(\text{OH})_3$) at the scratched area that suppress the dissolution of Fe from the bare steel. On the other hand, in the case of $\text{Ca}(\text{OH})_2$, the consumption of dissolved oxygen current ($I_{\text{oxv-c}}$) at the tip varied from 0.001 to 0.003 nA which was very less extent for 1 - 7 h immersion. Hence, the carbon steel did not effectively corrode in sat. $\text{Ca}(\text{OH})_2$ during the immersion of 1 - 7 h. Under these conditions, the well defined tip current distribution over the coated area (**Figure 6** and **Figure 7**) was observed which suggests that there was no under corrosion of steel-coating interface, since the consumption of dissolved oxygen occurs until at scratch area. Once the corrosion products are formed at scratch area, the ca-

thodic reactions were takes places at some other places particularly at scratch front where the direct diffusion of O_2 and aggressive ions (Cl^-) would occur.

3.2.2. SECM Analysis by Wet/Dry Corrosion Cycles Test

SECM 3D surface topographic images of scratched epoxy coated carbon steel after wet/dry corrosion cycles in sat. $Ca(OH)_2$ containing 3% NaCl at the tip potential at -0.70 V for 1 - 4 days are shown in **Figure 9**. It was found from **Figure 9(a)**; the well defined tip current distribution was observed at scratch area as well as coated area. The decrease in tip current distribution at scratch area indicates that consumption of dissolved oxygen could occur after 1st day of wet/dry corrosion cycle. However, the current distribution over the coating area could not changed much, which clearly shows there was no corrosion damage occurred over the coating effectively. Similar observation was also noticed for 2nd day of wet/dry corrosion cycle as shown in **Figure 9(b)**. However, there was additional corrosion sport (well defined decrease in tip current distribution) was observed along with the scratch front (arrow mark shown in **Figure 9(b)** right side). In addition, the slight decrease in tip current distribution was also observed at the same day of wet/dry corrosion cycle at away from the scratch (arrow mark shown in **Figure 9(b)** on left side), which was considered to be the formation of blister. The increase in wet/dry corrosion cycles from 2nd to 3rd day, the corrosion spot became a small (which was formed already in 2nd day on right side) along with formation of new corrosion spot (marked as a circle in **Figure 9(c)** right side) near the scratch front. At the same time, a new additional corrosion spot at away from the scratch (left side circle marked in **Figure 9(c)**) which was corresponds to the slight decrease in tip current distribution of 2nd day (arrow mark in **Figure 9(b)** on left side). There was an additional new corrosion spot could be observed on 3rd day, which was marked as triangle in **Figure 9(c)**. When increasing the wet/dry corrosion cycles to 4th day, the corrosion spot at away from the scratch (which was formed at 3rd day) showed decrease in tip current distribution, further which indicate the occurrence of corrosion (consumption of dissolved O_2). While the new corrosion spot formed under 3rd day (right side of the **Figure 9(c)**) became small which might be due to the formation of corrosion products by the rupture of the coating with increase in wet/dry corrosion cycles. The decrease in tip currents around the blisters along with original blister (acts as anodic zones) was attributed to the formation of corrosion products at center of blister which suppressed the diffusion of O_2 leads to the cathodic delamination around the

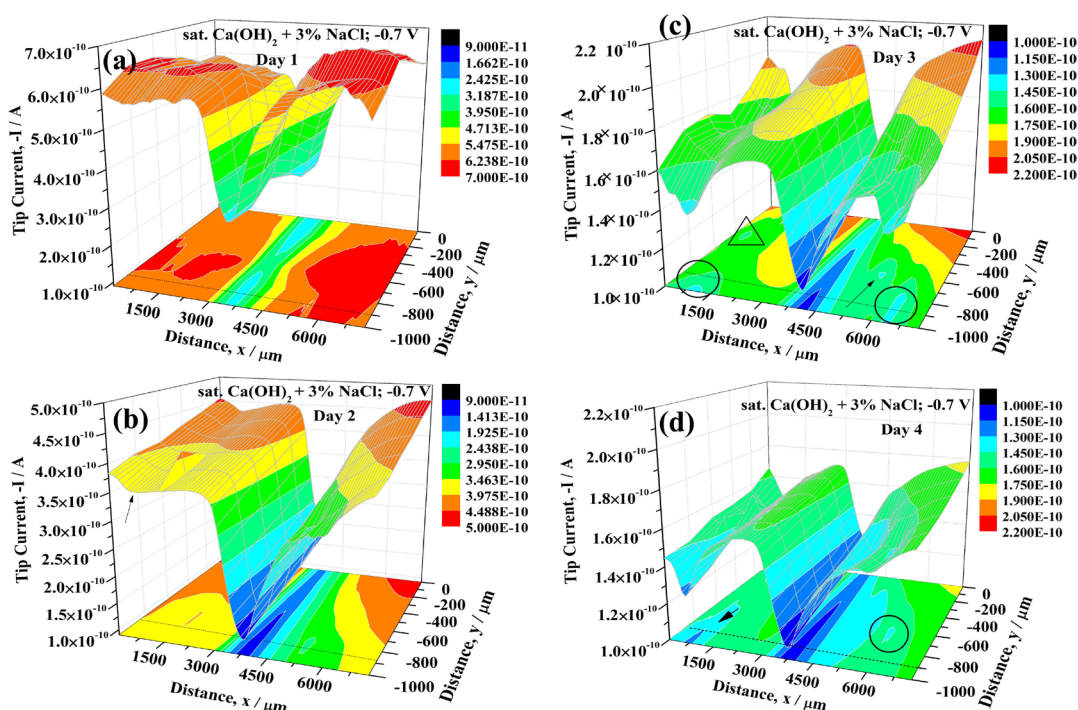


Figure 9. SECM topographic images of scratched epoxy coated carbon steel in sat. $Ca(OH)_2$ containing 3% NaCl after wet/dry corrosion test: (a) Day 1; (b) Day 2; (c) Day 3; and (d) Day 4 at the tip potential of -0.70 V vs. $Ag/AgCl/sat. KCl$. The images represent the $7000 \mu m \times 1000 \mu m$ in x and y directions. The vertical z direction is the tip current.

blister. The blister rupture could have occurred by repeated expansion-contraction under wet/dry cycles in which the metal surface was exposed to electrolyte directly (decrease in tip current equal to scratch area, blue color area marked as an arrow in **Figure 9(d)**) [9].

For better insight, the corresponding SECM line scans from **Figure 9** is examined for further analysis and shown in **Figure 10(a)** & **Figure 10(b)** at the specific regions (horizontal lines marked in **Figures 9(a)-(d)**). From **Figure 10(a)** & **Figure 10(b)** the tip current started to decrease at scratch from -0.255 to -0.115 nA for 1st to 3rd day of wet/dry corrosion cycle in Cl^- ion containing solution. The tip current was increased slightly (-0.129 nA) for 4th day of wet dry corrosion cycles. On the other hand, there was no change in tip currents could be observed at the scratch as well as in coated area except 4th day which shows the small fluctuations of tip current profile (Figs not shown) in sat. Ca(OH)_2 . The consumption of dissolved oxygen currents ($I_{\text{oxy-c}}$ and $I'_{\text{oxy-c}}$) at the scratch were given in **Figure 11(a)** for both solutions as discussed in section 3.2.1. It is seen from **Figure 11(a)**, the higher $I_{\text{oxy-c}}$ (-0.266 nA and -0.255 nA) for 1st and 2nd day of wet/dry cycles and sudden decrease in $I'_{\text{oxy-c}}$ (-0.056 nA and -0.047 nA) was observed for 3rd and 4th days of wet/dry corrosion cycles in sat. Ca(OH)_2 with 3% NaCl. This clearly indicates that consumption of dissolved oxygen was decreased considerably with increase in wet/dry corrosion cycles due to the formation of corrosion products that suppress the consumption of dissolved O_2 at the scratch area but not completely due to porous nature of the oxide layer. The well defined sharp decrease in tip current at scratch for 4th day suggests that the possibility of diffusion of O_2 could be accessed by the pores in the oxide film some extent. On the other hand, $I_{\text{oxy-c}}$ was almost zero (**Figure 11(a)**) in sat. Ca(OH)_2 , which means that complete passivation could occurred under wet/dry corrosion cycles and did not

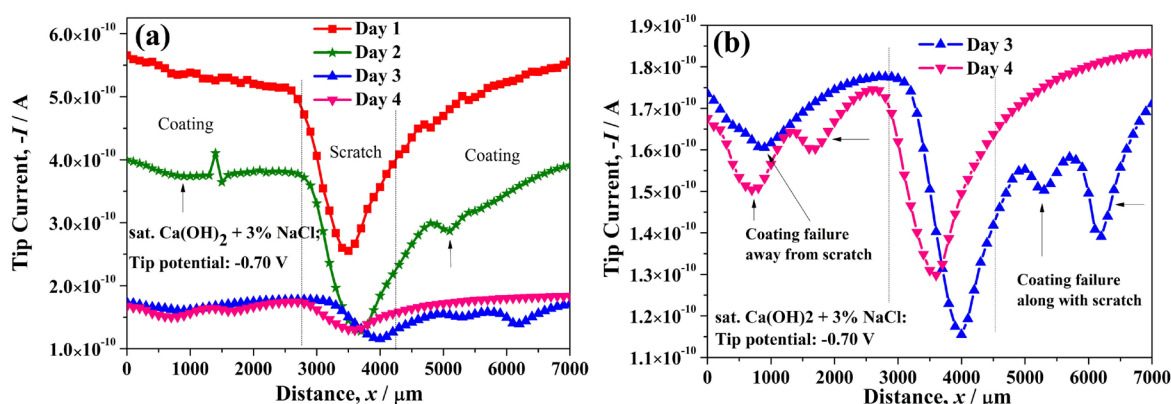


Figure 10. SECM line scans of scratched epoxy coated carbon steel in sat. Ca(OH)_2 containing 3% NaCl after wet/dry corrosion cycles for 1 - 4 days: (a) At tip potential: -0.70 V vs. Ag/AgCl/sat.KCl ; (b) expanded **Figure 10(a)** for day 3 and 4 respectively.

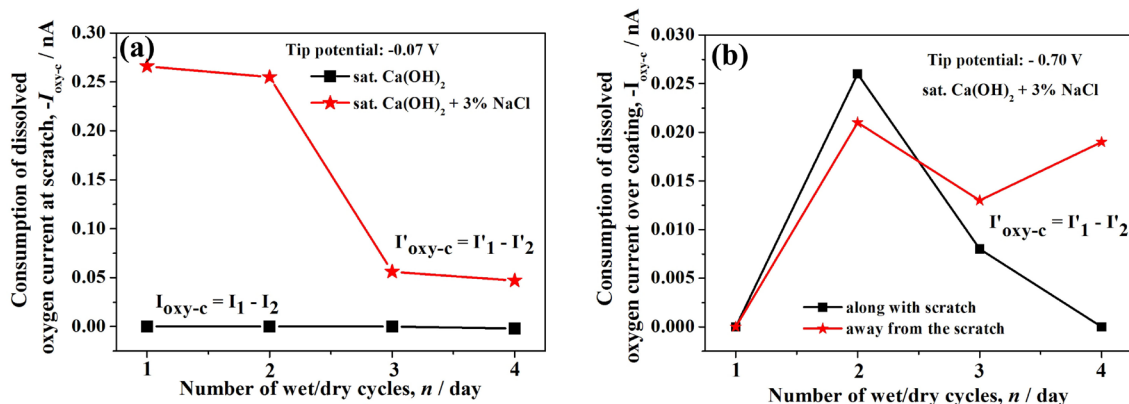


Figure 11. (a) Consumption of dissolved oxygen currents ($I_{\text{oxy-c}}$ and $I'_{\text{oxy-c}}$) at scratch area of epoxy coated carbon steel in in sat. Ca(OH)_2 and sat. Ca(OH)_2 containing 3% NaCl; (b) Consumption of dissolved oxygen current ($I'_{\text{oxy-c}}$) measured at corrosion spots along with scratch as well as away from the scratch in sat. Ca(OH)_2 containing 3% NaCl after wet/dry corrosion cycles for 1 - 4 days, at tip potential of -0.70 V vs. Ag/AgCl/sat.KCl respectively.

show the consumption of dissolved oxygen current ($I_{\text{oxy-c}}$). Hence, it is clear that increase of wet/dry corrosion cycles, the formation of corrosion products at scratch area which suppress the consumption of dissolved oxygen.

Once the corrosion products formed at scratch area, the oxygen diffusion could be restricted eventually the cathodic process could occur at some other place away from the scratch, which induced under-corrosion at steel-coating interface. This has been explained in **Figure 9(c)** that the formation of blisters around the scratch and away from the scratch. For better insight on these aspects, consumption of dissolved oxygen currents ($I_{\text{oxy-c}}$) measured over the corrosion spots (blisters) at the coating area along with scratch and away from the scratch were shown in **Figure 11(b)**. From **Figure 11(b)**, the higher $I_{\text{oxy-c}}$ for blister formation along with scratch front has been increased to -0.026 nA for 2nd day from day 1. Day 1 wet/dry cycles does not show any coating degradation since the corrosion occurs at scratch, the consumption dissolved O_2 was reduced at cathodic sites at steel surface (scratch area) rather than at coated area. The 3rd day to 4th day, the $I_{\text{oxy-c}}$ was decreased to large extent (-0.008 and 0 nA respectively) at blister due to the formation of corrosion products that suppressed the consumption of dissolved oxygen. In addition, the increase in $I_{\text{oxy-c}}$ (-0.026 nA) near the blister of 3rd day (-0.008 nA) was mainly due to the cathodic delamination. The formation of corrosion products at the blister acts as anodic zones that suppress the diffusion of O_2 and favors the reduction of O_2 at cathodic sites, especially around the blister, which in turn promotes cathodic delamination (marked as horizontal arrow mark in **Figure 11(b)**). On the other hand, the blister formation away from the scratch could also be observed with corresponding increase in $I_{\text{oxy-c}}$ (-0.020 nA) for 2nd day. At 3th day, $I_{\text{oxy-c}}$ was reduced from -0.020 nA to -0.013 nA, further it started to increase from -0.013 to -0.018 nA for 4th day (**Figure 9(d)** and **Figure 10(b)**). This might be due to the rupture of the blister during wet/dry corrosion cycles by repeated expansion-contraction in which steel surface was exposed to the electrolyte directly. The additional $I_{\text{oxy-c}}$ (-0.012 nA) along with already formed blister away from the scratch (marked as triangle in **Figure 9(c)**) has been also noticed which was due to the cathodic delamination (reduction of O_2 at cathodic sites around blister). These inferences clearly suggest that the corrosion could occur at the scratch as well as along with the scratch via anodic blistering due to direct penetration of electrolyte as well as diffusion of oxygen and Cl^- ions [10]. The cathodic blistering is occurred at away from the scratch, because of the formation of corrosion products at the scratch area or other anodic zones with time that hinders the diffusion of O_2 . Consequently, the cathodic reactions can take place away from the scratch, which in turn promotes the formation of cathodic blister by cathodic reactions at steel-coating interface. The increase in wet/dry corrosion cycles, diffusion of oxygen and Cl^- ion penetration leads to the formation of anodic zones at center of the blister and cathodic areas around the anodic zones which eventually separates the anodic and cathodic areas inside the cathodic blister [17]. With increase in wet/dry corrosion cycles further, corrosion products formed at anodic zones and cathodic delamination would increase within the blister. This in turn promotes the osmotic pressure that ruptures the already formed blisters due to the repeated expansion-contraction under drying cycles and the blister formation could be extended some other places.

4. Corrosion Mechanism of Scratched Epoxy Coated Carbon Steel

Based on the inferences made in the present study, the graphical model is proposed to understand the local degradation of coating and steel corrosion at scratch of epoxy coated carbon steel in sat. $\text{Ca}(\text{OH})_2$ containing 3% NaCl (**Figure 12**). In open circuit potential, the anodic, metal dissolution reaction is balanced by the cathodic process of oxygen reduction reaction at steel surface (scratched area). In wet process (immersion), the increase in $I_{\text{oxy-c}}$ at scratched area up to 4 h immersion and started to decrease gradually after 4 h immersion in sat. $\text{Ca}(\text{OH})_2$ containing 3% NaCl (**Figure 8**). This supports the formation of hydroxides ($\text{Fe}(\text{OH})_2$ or $\text{Fe}(\text{OH})_3$) at the scratched area as shown in **Figure 12(a)**. The formation of these hydroxides at the scratch area suppressed the transport of O_2 at this defect site and favors the reduction of O_2 at cathodic sites, especially at the scratch front, which in turn promoted the cathodic delamination (**Figure 11(a)**). Wet/dry corrosion cycle's performance result showed that the corrosion at the scratch area as well as at scratch front and coated area (**Figure 9** and **Figure 10**) has been shown in **Figure 12(b)**. Under wet/dry corrosion cycles, the FeOOH could be formed at the scratch area in the presence oxygen, while green rust ($\text{GR}(\text{Cl}^-)$) might be formed intermediately at the interface of Fe and FeOOH . At the same time, in the presence oxygen, $\text{GR}(\text{Cl}^-)$ could be easily converted into FeOOH due to the less stability of $\text{GR}(\text{Cl}^-)$ [18].

Park *et al.* [17] has reported that the epoxy coating without defect in 0.5 M NaCl, the blister formation was responsible for the under steel corrosion via osmotic blistering due to the water uptake with contamination (salts).

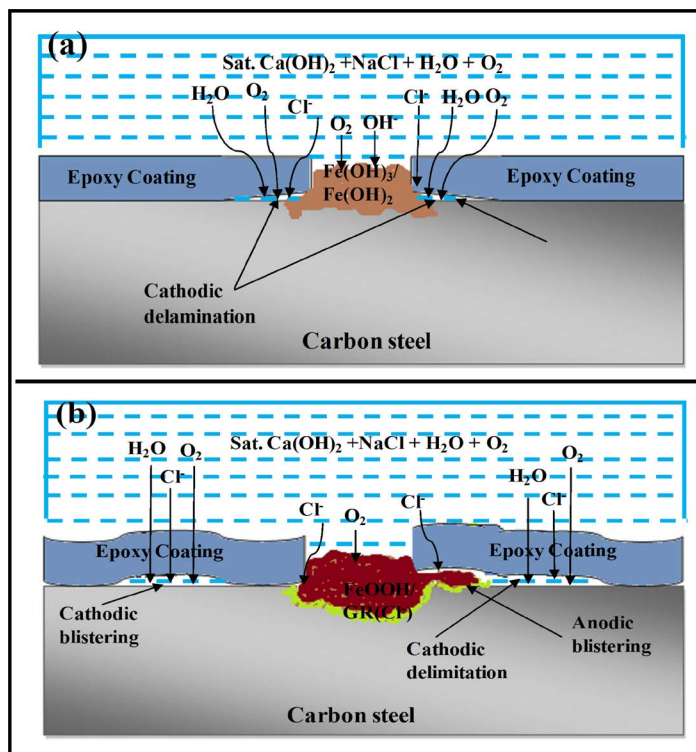


Figure 12. Graphical representation depicting the mechanism of scratched epoxy coated carbon steel in sat. Ca(OH)_2 containing 3% NaCl: (a) 1 - 7 h immersion ; (b) 1 - 4 days of wet/dry corrosion cycles.

In such case, under corrosion of steel was due to intake of water and diffusion of dissolved oxygen that separates the anodic and corresponding cathodic reactions within a blister. Once the corrosion products are formed at the blister region, the oxygen diffusion could be restricted and eventually the cathodic process could occur at some other place away from the original blister, which would be termed as cathodic blister formation. Hence, in the present study, the formation of blisters along with the scratch was termed as anodic blisters by the direct penetration of Cl^- ions and O_2 diffusion through scratch front that produces anodic zones/corrosion products. This induced blister formation at steel-coating interface (**Figure 12(b)**). This has been clearly observed in our recent study [19] by laser microscopic observation of epoxy coated SM (carbon steel) with crosscuts. It was found that many corrosion pits around the scratch area in 0.1 M NaCl after 14 days of wet/dry corrosion test. The formation of blisters away from the scratch could be termed as cathodic blisters when the coating has considerable artificial defect (**Figure 12(b)**). Cathodic blisters could be formed due to the cathodic reactions, when the scratch area was filled with the corrosion products which suppress diffusion of O_2 and the cathodic reaction could be shifted to some other places which promote the cathodic delamination. This process has been continued with increase in wet/dry corrosion cycle's leads to the continuous decrease in corrosion resistance of scratched epoxy coated carbon steel in sat. Ca(OH)_2 containing 3% NaCl. The results observed from the EIS and SECM studies corroborate well with each other that the corrosion at scratch as well as along with scratch and away from the scratch via blistering.

5. Conclusions

The effect of 3% NaCl in sat. Ca(OH)_2 on the local corrosion process of scratched epoxy coated carbon steel was studied by SECM and correlated with EIS. The EIS results showed that the decrease in film resistance (R_f) from 1.0 to 0.14 $\text{k}\Omega\cdot\text{cm}^2$ in sat. Ca(OH)_2 with 3% NaCl with increase in wet/dry corrosion cycles for 1 - 15 days, while they were sustained the resistance values (15.22 $\text{k}\Omega\cdot\text{cm}^2$) in an absence of Cl^- ions. The charge transfer resistance (R_{ct}) of corroded steel in the presence of Cl^- ions was decreased to large extent from 61.19 to 4.48 $\text{k}\Omega\cdot\text{cm}^2$, while the decrease in R_{ct} values (2.42 to 0.77 $\text{M}\Omega\cdot\text{cm}^2$) was marginal in saturated Ca(OH)_2 . It was seen visually that numerous corrosion spots at away from the scratch were responsible for continuous decrease in

corrosion resistance in Cl^- containing solution, which induced an additional pathways for corrosion. The resistance values of scratched epoxy coated carbon steel did not change significantly in absence of Cl^- ions due the recovery of coating properties after drying.

For better insight on the extent of local corrosion attack around the scratch, epoxy coated steel was observed using SECM in immersion and wet/dry corrosion cycles test in sat. $\text{Ca}(\text{OH})_2$ with and without 3% NaCl. The SECM tip potential was set at -0.70 V vs Ag/AgCl, where the consumption of dissolved oxygen ($I'_{\text{oxy-c}}$) occurred at the surface of test sample. SECM test results based on $I'_{\text{oxy-c}}$ revealed that the corrosion started at scratch and spread further away from the scratch (coated area). During immersion, the $I'_{\text{oxy-c}}$ values were increased from -0.027 to -0.079 nA for 1 - 4 h and it decreased to -0.051 nA with 7 h immersion. Besides, in wet/dry corrosion cycles, $I'_{\text{oxy-c}}$ was decreased at scratch area from -0.266 nA (1st day) to -0.047 nA (4th day) in saturated $\text{Ca}(\text{OH})_2$ with 3% NaCl solution. This behavior was due to the covering effect of hydroxides/oxides which constrained the consumption of dissolved O_2 . However, the new anodic spots at away from the scratch were caused the degradation of coating which was due to cathodic reactions. It was found that the corrosion was suppressed by the formation of corrosion products at the scratch. Besides, the continuous decrease in corrosion resistance was also observed due to the creation of new anodic spots, which caused the degradation of the epoxy coating. The experimental results obtained from SECM were good agreement with EIS and visual observations in sat. $\text{Ca}(\text{OH})_2$ with 3% NaCl.

Acknowledgements

This work was supported by Council for Science, Technology and Innovation (CSTI), Cross-ministerial Strategic Innovation Promotion Program (SIP), “Infrastructure maintenance, renovation and management” (Funding agency: JST).

References

- [1] Souto, R.M., González-García, Y., González, S. and Burstein, G.T. (2014) Damage to Paint Coatings Caused by Electrolyte Immersion as Observed *in Situ* by Scanning Electrochemical Microscopy. *Corrosion Science*, **46**, 2621-2628. <http://dx.doi.org/10.1016/j.corsci.2004.06.002>
- [2] Schaller, R.F., Thomas, S., Birbilis, N. and Scully, J.R. (2015) Spatially Resolved Mapping of the Relative Concentration of Dissolved Hydrogen Using the Scanning Electrochemical Microscope. *Electrochemistry Communications*, **51**, 54-58. <http://dx.doi.org/10.1016/j.elecom.2014.12.004>
- [3] Meyer, J.N., Mathew, M.T., Wimmer, M.A. and Le Suer, R.J. (2013) Effect of Tribolayer Formation on Corrosion of CoCrMo Alloys Investigated Using Scanning Electrochemical Microscopy. *Analytical Chemistry*, **85**, 7159-7166. <http://dx.doi.org/10.1021/ac400823q>
- [4] Souto, R.M., González-García, Y. and González, S. (2005) *In Situ* Monitoring of Electroactive Species by Using the Scanning Electrochemical Microscope. Application to the Investigation of Degradation Processes at Defective Coated Metals. *Corrosion Science*, **47**, 3312-3323. <http://dx.doi.org/10.1016/j.corsci.2005.07.005>
- [5] Bastos, A.C., Simões, A.M., González, S., González-García, Y. and Souto, R.M. (2004) Imaging Concentration Profiles of Redox-Active Species in Open-Circuit Corrosion Processes with the Scanning Electrochemical Microscope. *Electrochemistry Communications*, **6**, 1212-1215. <http://dx.doi.org/10.1016/j.elecom.2004.09.022>
- [6] Abodi, L.C., Gonzalez-Garcia, Y., Dolgikh, O., Dan, C., Deconinck, D., Mol, J.M.C., Terryn, H. and Deconinck, J. (2014) Simulated and Measured Response of Oxygen SECM-Measurements in Presence of a Corrosion Process. *Electrochimica Acta*, **146**, 556-563. <http://dx.doi.org/10.1016/j.electacta.2014.09.010>
- [7] Izquierdo, J., Nagy, L., González, S., Santana, J.J., Nagy, G. and Souto, R.M. (2013) Resolution of the Apparent Experimental Discrepancies Observed between SVET and SECM for the Characterization of Galvanic Corrosion Reactions. *Electrochemistry Communications*, **27**, 50-53. <http://dx.doi.org/10.1016/j.elecom.2012.11.002>
- [8] Fernández-Pérez, B.M., Izquierdo, J., González, S. and Souto, R.M. (2014) Scanning Electrochemical Microscopy Studies for the Characterization of Localized Corrosion Reactions at Cut Edges of Coil-Coated Steel. *Journal of Solid State Electrochemistry*, **18**, 2983-2992. <http://dx.doi.org/10.1007/s10008-014-2397-z>
- [9] Schachinger, E.D., Braidt, R., Strauß, B. and Hassel, A.W. (2015) EIS Study of Blister Formation on Coated Galvanised Steel in Oxidising Alkaline Solutions. *Corrosion Science*, **96**, 6-13. <http://dx.doi.org/10.1016/j.corsci.2014.12.010>
- [10] Nguyen, T. and Martin, J.W. (2004) Modes and Mechanisms for the Degradation of Fusion-Bonded Epoxy-Coated Steel in a Marine Concrete Environment. *Journal of Coatings Technology and Research*, **1**, 81-92.

<http://dx.doi.org/10.1007/s11998-004-0002-6>

- [11] Dong, Y. and Zhou, Q. (2014) Relationship between Ion Transport and the Failure Behavior of Epoxy Resin Coatings. *Corrosion Science*, **78**, 22-28. <http://dx.doi.org/10.1016/j.corsci.2013.08.017>
- [12] Vakili, H., Ramezanzadeh, B. and Amini, R. (2015) The Corrosion Performance and Adhesion Properties of the Epoxy Coating Applied on the Steel Substrates Treated by Cerium-Based Conversion Coatings. *Corrosion Science*, **94**, 466-475. <http://dx.doi.org/10.1016/j.corsci.2015.02.028>
- [13] Madhankumar, A., Nagarajan, S., Rajendran, N. and Nishimura, T. (2012) EIS Evaluation of Protective Performance and Surface Characterization of Epoxy Coating with Aluminum Nanoparticles after Wet and Dry Corrosion Test. *Journal of Solid State Electrochemistry*, **16**, 2085-2093. <http://dx.doi.org/10.1007/s10008-011-1623-1>
- [14] Grousset, S., Kergourlay, F., Neff, D., Foy, E., Gallias, J.L., Reguer, S., Dillmann, P. and Noumowé, A. (2015) *In Situ* Monitoring of Corrosion Processes by Coupled Micro-XRF/Micro-XRD Mapping to Understand the Degradation Mechanisms of Reinforcing Bars in Hydraulic Binders from Historic Monuments. *Journal of Analytical Atomic Spectrometry*, **30**, 721-729. <http://dx.doi.org/10.1039/C4JA00370E>
- [15] Lin, B., Hu, R., Ye, C., Li, Y. and Lin, C. (2010) A Study on the Initiation of Pitting Corrosion in Carbon Steel in Chloride-Containing Media Using Scanning Electrochemical Probes. *Electrochimica Acta*, **55**, 6542-6545. <http://dx.doi.org/10.1016/j.electacta.2010.06.024>
- [16] Balusamy, T. and Nishimura, T. (2016) *In-Situ* Monitoring of Local Corrosion Process of Scratched Epoxy Coated Carbon Steel in Simulated Pore Solution Containing Varying Percentage of Chloride Ions by Localized Electrochemical Impedance Spectroscopy. *Electrochimica Acta*, **199**, 305-313. <http://dx.doi.org/10.1016/j.electacta.2016.02.034>
- [17] Park, J.H., Lee, G.D., Ooshige, H., Nishikata, A. and Tsuru, T. (2003) Monitoring of Water Uptake in Organic Coatings under Cyclic Wet-Dry Condition. *Corrosion Science*, **45**, 1881-1894. [http://dx.doi.org/10.1016/S0010-938X\(03\)00024-6](http://dx.doi.org/10.1016/S0010-938X(03)00024-6)
- [18] Génin, J.M.R., Dhoubi, L., Refait, Ph., Abdelmoula, M. and Triki, E. (2002) Influence of Phosphate on the Corrosion Products of Iron in Chloride-Polluted Concrete-Simulating Solutions: Ferrihydrite vs Green Rust. *Corrosion*, **58**, 467-478. <http://dx.doi.org/10.5006/1.3277637>
- [19] Nishimura, T. (2016) Corrosion Estimation of Epoxy Coated High Tensile Strength Steel Measured by Statistical Analysis and TEM-EELS. *Materials Transactions*, **57**, 52 -57. <http://dx.doi.org/10.2320/matertrans.M2015241>



Submit or recommend next manuscript to SCIRP and we will provide best service for you:

Accepting pre-submission inquiries through Email, Facebook, LinkedIn, Twitter, etc
A wide selection of journals (inclusive of 9 subjects, more than 200 journals)
Providing a 24-hour high-quality service
User-friendly online submission system
Fair and swift peer-review system
Efficient typesetting and proofreading procedure
Display of the result of downloads and visits, as well as the number of cited articles
Maximum dissemination of your research work

Submit your manuscript at: <http://papersubmission.scirp.org/>